Journal of Structural Geology 105 (2017) 80–87

Contents lists available at ScienceDirect

Journal of Structural Geology

journal homepage: www.elsevier.com/locate/jsg

Stress dependence of microstructures in experimentally deformed calcite

John P. Platt[a,*], J.H.P. De Bresser[b]

[a] Department of Earth Sciences, University of Southern California, Los Angeles, CA, 90089-0742, USA
[b] HPT-laboratory, Department of Earth Sciences, PO Box 80.021, 3508 TA, Utrecht University, The Netherlands

ARTICLE INFO

Keywords:
Dynamically recrystallized grain-size
Subgrain
Grain-boundary migration
Lattice strain energy
Grain-boundary energy

ABSTRACT

Optical measurements of microstructural features in experimentally deformed Carrara marble help define their dependence on stress. These features include dynamically recrystallized grain size (*Dr*), subgrain size (*Sg*), minimum bulge size ($L\rho$), and the maximum scale length for surface-energy driven grain-boundary migration ($L\gamma$). Taken together with previously published data *Dr* defines a paleopiezometer over the range 15–291 MPa and temperature over the range 500–1000 °C, with a stress exponent of −1.09 (CI −1.27 to −0.95), showing no detectable dependence on temperature. *Sg* and *Dr* measured in the same samples are closely similar in size, suggesting that the new grains did not grow significantly after nucleation. $L\rho$ and $L\gamma$ measured on each sample define a relationship to stress with an exponent of approximately −1.6, which helps define the boundary between a region of dominant strain-energy-driven grain-boundary migration at high stress, from a region of dominant surface-energy-driven grain-boundary migration at low stress.

1. Introduction

Plastic deformation of crystalline solids produces distinctive and informative microstructures (e.g., White, 1976). These include lattice distortion, which reflects the density of lattice defects; low-angle tilt and twist boundaries within grains, which reflect the operation of recovery processes such as dislocation climb; and dynamic recrystallization, which reflects a variety of processes that produce new grains as well as the migration of grain-boundaries driven by lattice strain energy and grain-boundary surface energy (Karato, 1988; Hirth and Tullis, 1992). Features such as the crystallographic preferred orientation, dynamically recrystallized grain size, subgrain size, twin density, and dislocation density can provide a wealth of information, both about the slip systems active during deformation (Lloyd et al., 1997; Halfpenny et al., 2006), and on the physical conditions during deformation. Experimental deformation under controlled conditions can provide calibrations of the relationships between microstructural features and deformational parameters including temperature (e.g., Barnhoorn et al., 2004; ter Heege et al., 2005), water content (e.g., Jung and Karato, 2001; Stipp and Tullis, 2006), and differential stress (e.g. Karato et al., 1980; van der Wal et al., 1993; Post and Tullis, 1999; Stipp and Tullis, 2003; Siemes et al., 2011; Kidder et al., 2016; Cross et al., 2017).

A substantial amount of experimental work has been done on calcite marble from the Carrara quarries in the northern Italian Apennines, because of its purity, homogeneity, and lack of significant shape or crystallographic fabric (Schmid et al., 1980; Rutter, 1995; Pieri et al., 2001a, 2001b; ter Heege et al., 2002; Barnhoorn et al., 2004; De Bresser et al., 2005), and these experiments have provided information on the rheological properties, deformational mechanisms, and microstructural processes of calcite in general and Carrara marble in particular. Deformed samples from a series of experiments carried out at Utrecht University, the Netherlands (ter Heege et al., 2002; De Bresser et al., 2005) and ANU Canberra, Australia (De Bresser et al., 2005) were archived, and some were subsequently studied in detail by Valcke et al. (2006, 2007, 2014) who documented microstructural relationships among deformed grains, dynamically recrystallized grains, subgrains, and grain-boundary bulges. This paper builds on these studies, with the specific aim of testing recently developed hypotheses about dynamic recrystallization, nucleation, and grain-size evolution (De Bresser et al., 1998; Shimizu, 1998; De Bresser et al., 2001; Kellermann Slotemaker and De Bresser, 2006; Austin and Evans, 2007, 2009; Platt and Behr, 2011; Herwegh et al., 2014).

A particular goal of this work was to locate the boundary in stress/grain-size space between the regions where lattice strain energy and surface energy respectively provide the dominant driver for grain-boundary migration. These two regions should show significantly different microstructures, and grain growth is only likely to occur in the region where surface energy dominates (Platt and Behr, 2011). This line, known as the D_{min} line, is predicted on theoretical grounds to be temperature independent, with a slope of 2 in log stress/log grain-size space, but as far as we know it has not been confidently located for any material.

* Corresponding author.
E-mail address: jplatt@usc.edu (J.P. Platt).

https://doi.org/10.1016/j.jsg.2017.10.012
Received 27 June 2017; Received in revised form 29 October 2017; Accepted 30 October 2017
Available online 16 November 2017

Table 1
Experimental and microstructural data. ln(e), natural strain. Stress is differential stress at the end of the experiment, except for 36LM900 (starred), for which it is the average of the stresses measured at the end of the first three of four strain steps. *Dr*, dynamically recrystallized grain size (RMS of equivalent circle diameter). *Sg*, subgrain size, measured in the same way as *Dr*. *Lρ*, minimum diameter of viable bulges. *Lγ*, maximum scale length of surface-energy driven grain-boundary migration. Samples coded LM from ter Heege et al. (2002), the other samples from De Bresser et al. (2005). See text for further explanation.

Sample #	% axial shortening	ln(e)	T°C	stress MPa	*Dr μm*	± *Dr* (*n*)	*Sg μm*	± *Sg* (*n*)	*Lρ*	*Lγ*
15LM950	36	−0.45	962	14.6	79	23 (72)	72	21 (50)	46	58
25LM950	36	−0.45	950	24.8	31.6	12 (39)	23.9	15 (36)	12	10
23LM900	36	−0.45	900	21.8	43	13 (33)	35	13 (19)	10.8	11
36LM900	59	−0.9	900	34.4*	13.9	5 (41)	13.9	5 (26)	7	9
50LM900	36	−0.45	900	44.4	36	13 (47)	37	11 (7)	7	11
50LM780	36	−0.45	780	47.3	13.5	7 (25)	13.1	5 (27)	3	4
50LM730	36	−0.45	730	52.1	13.8	2 (30)	11	3 (22)	4.5	7
65LM700	36	−0.45	700	65.0	14.1	2 (49)	10.5	3 (29)	4	6
85LM730	36	−0.45	730	82.1			5.2	2 (13)	2	
5347	21	−0.24	1000	27.5	41	14 (29)	43	25 (15)	16	13
5356	21	−0.24	1000	21.6	34	12 (71)	30	13 (11)	13	13
5348	20	−0.22	800	63.9	22	9 (39)	22	11 (39)	6.6	7.3
5321	10	−0.11	800	45.8	33	15 (33)	30	15	8	10
5325	13	−0.14	800	44.5	25	10 (50)	32	15	8	9
5332	26	−0.30	800	71.4	20	7 (35)	22	11	3	4.5

2. Methods

The original experiments were carried out in axial compression by constant displacement rate tests in a constant volume, internally heated argon gas-medium apparatus (Utrecht University or ANU Canberra) under a confining pressure of 300 MPa to natural strains of 0.15–0.90 at strain rates of 3×10^{-6} to 4.9×10^{-4} s^{-1} and temperatures of 700–1000 °C (ter Heege et al., 2002; De Bresser et al., 2005). The samples were rapidly quenched after deformation to preserve the microstructures. Differential stresses during the experiments ranged from 15 to 90 MPa. In most experiments stress reached a peak at a natural strain of 0.02–0.1, and then progressively dropped by up to 12 MPa during deformation. As discussed later, for all but one of the experiments we have used the final stress when assessing the significance of the microstructures. Temperature and stress during deformation for the samples we analyzed are shown in Table 1.

Electron backscatter diffraction analysis (EBSD) on the scanning electron microscope is increasingly used as the technique of choice for microstructural analysis of deformed mineral aggregates (e.g., Prior et al., 1999, 2009), and was the basis for the studies of Valcke et al. (2006, 2007 and 2014). EBSD has several clear advantages; it provides higher resolution than optical studies; it allows grains and subgrains to be distinguished precisely in terms of their complete crystallographic orientation and their lattice misorientation with respect to their neighbours; and it provides maps that can be rapidly analyzed in terms of grain size and grain shape.

Other techniques that may be appropriate in particular situations include traditional optical microscopy and etching of polished surfaces. A distinctive feature of calcite is that its high birefringence means that thin-sections as little as 5 μm thick show first-order interference colours under the optical microscope, which allows optical study of features at scales that are only limited by the wavelength of light (~0.5 μm). The sharp relief contrast on grain boundaries allows features such as grain-boundary bulges to be imaged very precisely, and the ability of the microscope to focus through the thickness of the section means that the 3-D geometry of such features can be characterized effectively. As discussed below, two of the principle aims of this study were to measure the minimum size of grain-boundary bulges *Lρ*, and the scale length *Lγ* of grain-boundaries that have been modified by surface-energy-driven grain boundary migration (referred to here as γ-GBM, after Platt and Behr, 2011) (Fig. 1). Both these features are difficult to identify and measure with EBSD unless very small step sizes are used, which places practical limits on the area that can be examined in detail. Optical microscopy allows large areas to be scanned rapidly for pertinent microstructures, which can then be studied at high resolution. For these reasons, this study was carried out on using optical microscopy on ultra-thin sections.

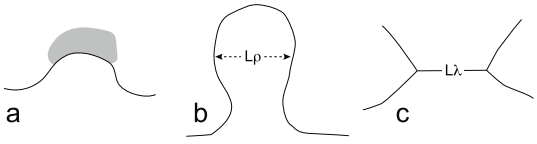

Fig. 1. a) Sketch of a grain boundary bulge that has not amplified much. This may be transient, driven by a local region of high dislocation density, and hence liable to shrinkage and elimination driven by γ-GBM. b) Sketch of a grain-boundary bulge that has amplified to the point that its length is greater than its diameter. This is likely to indicate that amplification is driven by the ambient average dislocation density, and hence that the bulge is likely to survive. The minimum size of such bulges defines the scale length *Lρ* of ρ-GBM. c) Sketch of a straight grain-boundary bounded by ~120° triple junctions. The length of the grain-boundary defines the scale length of γ-GBM.

A challenging aspect of studying the process of dynamic recrystallization in experimentally deformed samples that have only reached low strains, and hence low proportions of new grains, is distinguishing new grains from the remnants of the original grains, which may be dissected by kink-bands, twins, fractures, or micro-scale shear zones. The study by Valcke et al. (2014), for example, placed particular importance on the use of EBSD for the identification of recrystallized grains based on their lack of substructure (lattice distortion and subgrains), which provides a systematic and objective criterion for microstructural description. A potential problem with this approach is that in a deforming medium, some new grains may have a significant dislocation density, and hence may show lattice distortion and small-scale dislocation cells or subgrains. One reason for this is that new grains formed by the subgrain rotation mechanism (SGR) are likely to have a dislocation density, and hence lattice misorientation, comparable to their parent grains. Also, new grains formed by the grain-boundary bulging mechanism (BLG) may have low dislocation densities initially, but this makes them relatively soft, so they deform more rapidly than the bulk aggregate, and their dislocation density increases rapidly after nucleation (Humphreys and Hatherly, 2004). The net result is that many recrystallized grains are likely to be overlooked, with unpredictable effects on the resulting grain-size distribution.

Optical microscopy allows an alternative approach to the definition of recrystallized grains that may lead to somewhat different results and insights. New grains can be identified based on a number of microstructural criteria that can be rapidly determined by inspection under the optical microscope. In many samples, recrystallized grains form aggregates of sub-equant grains that are distinctly smaller than relict primary grains, and have more regular shapes than dissected remnants

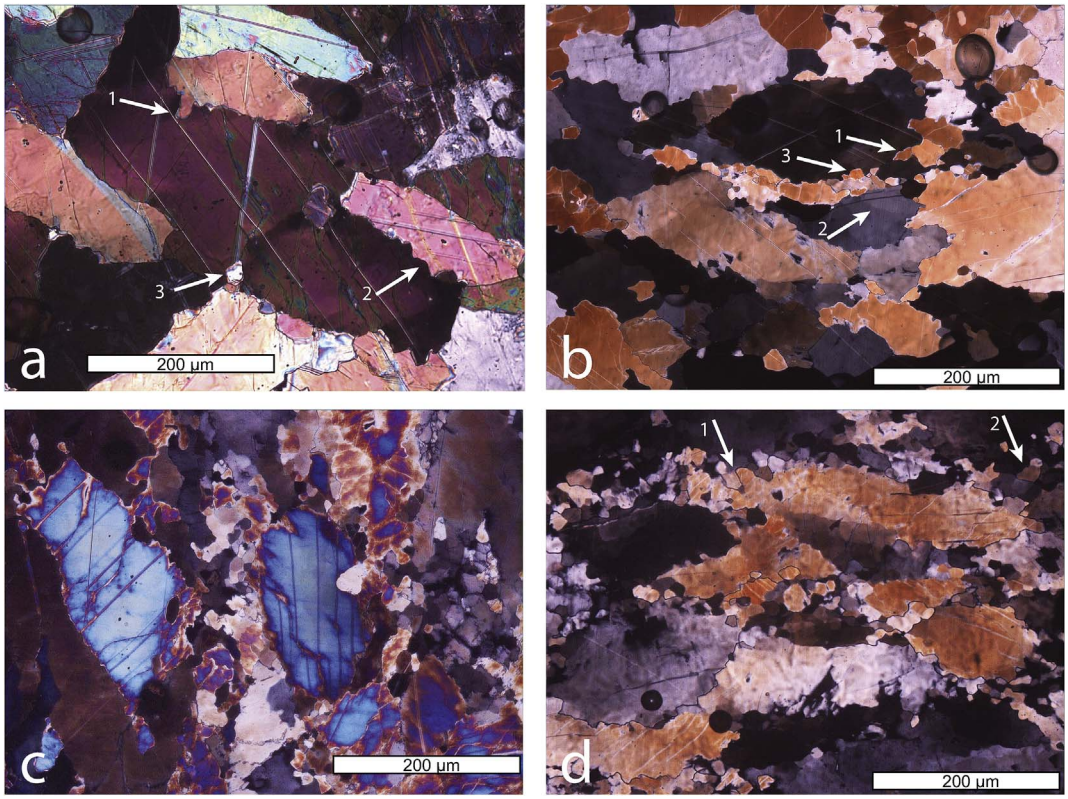

Fig. 2. Photomicrographs of experimentally deformed calcite taken in cross-polarized light on ultrathin sections (~5 μm), showing mechanisms and microstructures of dynamic recrystallization. a) Grain-boundary bulges. Arrow 1, bulge has amplified to the point that it can survive, and was measured; lower amplitude bulges (e.g., arrow 2) are likely to be transient. Arrow 3, new grains formed by BLG. Sample 25LM950 (24.8 MPa, 950 °C). b) Bulges (arrow 1), subgrain boundaries (arrow 2), and incipient nucleation of new grains by BLG and SGR (arrow 3). Sample 50LM780 (47.3 MPa, 780 °C). c) Primary grains dissected by chains of new grains formed by BLG and SGR. Sample 50LM730 (52.1 MPa, 730 °C). d) Extensive dissection of primary grains by new grains formed by BLG (arrow 1) and SGR (arrow 2). Grains nucleated by both mechanisms show irregular grain boundaries and bulge into adjacent grains. Sample 36LM900 (34.4 MPa, 900 °C).

of old grains (Fig. 2c and d, 3a). New grains formed by the BLG and SGR mechanisms have distinctive morphologies and relations to the primary grains that allow ready identification (Fig. 2b and d, 3b and c). New grains can be distinguished from subgrains not only by misorientation, but because subgrains tend to have relatively straight boundaries (indicated by white arrows in Fig. 3c), whereas new grains tend to have curved boundaries due to strain-energy-driven grain-boundary migration (referred to here as ρ-GBM, after Platt and Behr, 2011). These criteria are to some extent subjective, and are not infallible, but are the same as used by Stipp and Tullis (2003), for example, when calibrating the quartz paleopiezometer. They allow fairly rapid identification of recrystallized grains on the scale of a thin-section, and they avoid the difficulties presented by the use of lattice distortion as a criterion.

In most samples, the recrystallization mechanism appears to be a combination of BLG and SGR, including bulges that are separated from the parent grain by a subgrain boundary, bulges pinned by subgrain boundaries, and grains formed by SGR that have then bulged back into the parent grain. Some of the highest stress samples seem to have recrystallized mainly by BLG, but none seem to been recrystallized purely by SGR. A few higher temperature and lower stress samples show “Regime 3” type (GBM) microstructures: large irregular grains have interlocking grain boundaries produced by grain-boundary migration, with only limited amounts of nucleation (Figs. 3d and 4). In these samples, we only measured grains that are clearly new, rather than the large interpenetrating grains that may be relict primary grains.

Grain size was estimated by measuring the long and short axes of grains (approximated as ellipses), and taking the square root of the product as the diameter of the equivalent circle. No stereological correction was applied, for consistency with previous studies. The mean grain size for each sample was calculated as the root mean square (RMS) of the data.

In addition to the dynamically recrystallized grain size, subgrain diameters were measured within deformed old grains. As pointed out by Valcke et al. (2006, 2007), there is a hierarchy of subgrains with misorientations varying from 0.5° to 10°, and a tendency for subgrains to be smaller near the rims of grains than in the cores. Above 10°, Valcke et al. (2006) did not see a hierarchy, and the grains were treated as recrystallized grains. For the purposes of this paper, only subgrains with misorientations large enough to be clearly visible in the optical microscope were measured, for comparison to the dynamically recrystallized grain-size in the same sample.

Two further types of microstructural measurement were made on each sample.

1) We measured the diameter of the smallest grain-boundary bulge that has amplified to the point that its length is greater than its diameter (Figs. 1b, 2a and 3b and d). This geometry ensures that the bulge was not a transient feature that could be eliminated during deformation by shrinkage driven by γ-GBM. There is a danger that the size of the smallest bulge could be under-estimated because of the cut effect, but this effect is not likely to be large, because oblique cuts through elongate bulges are likely to produce isolated grain "islands" in 2-D, which we did not measure.
2) We also measured the scale length at which grain-boundaries show evidence of modification by γ-GBM. This scale length is defined as the length of a straight boundary that connects two triple points with interfacial angles in two dimensions of ~120° (Figs. 1c, 3d and 4).

The rationale behind these measurements is they should bracket the

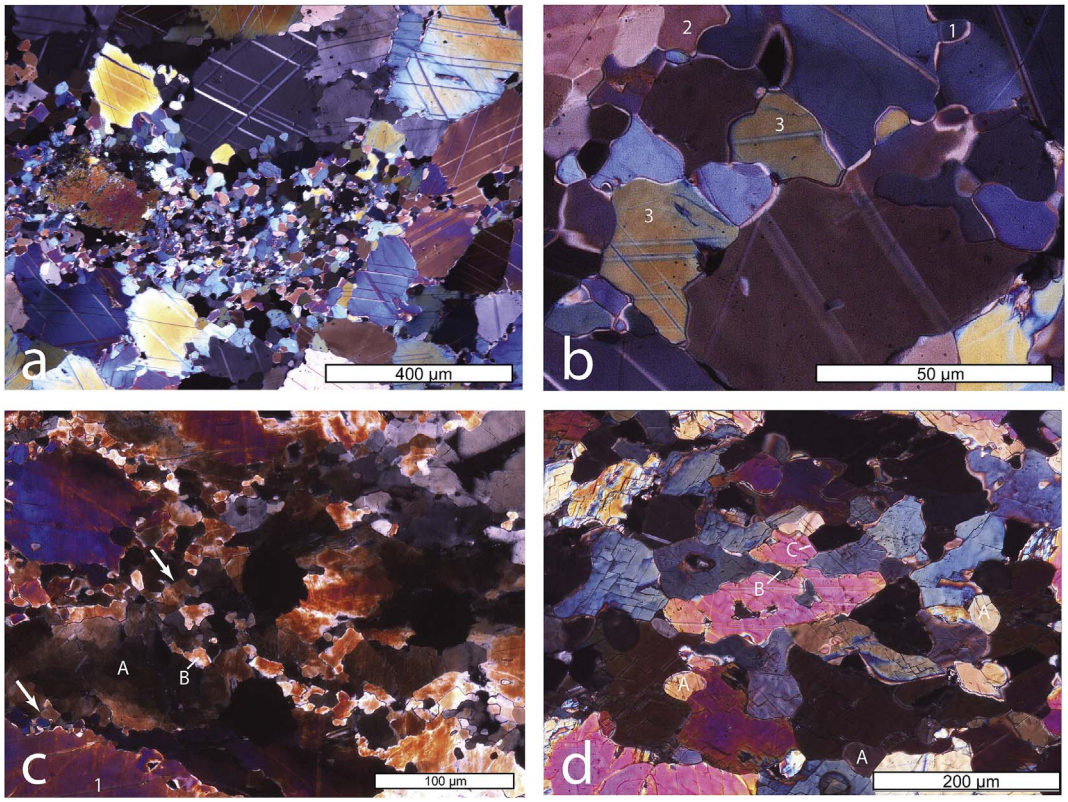

Fig. 3. High stress microstructures. a) Extensive aggregate of dynamically recrystallized grains surrounded by relict primary grains. New grains have a limited size range, and are distinct from the much larger primary grains. Sample 5325 (44.5 MPa, 800 °C). b) Enlarged view of sample 5325 showing new grains formed by BLG (grain 1) and SGR (grain 2). Grains labelled 3 may be dismembered relics of a primary grain. All grain boundaries have been modified by ρ-GBM. c) Large primary grains (e.g., A) have extensive subgrain structure, leading to aggregates of new grains produced by SGR (e.g., B). New grains have irregular (bulged) grain-boundaries, in contrast to more regular subgrain boundaries (white arrows). Subgrains, and new grains produced by BLG and SGR, have similar sizes. Sample 65LM700 (65 MPa, 700 °C). d) Microstructure produced by extensive GBM without much nucleation in an aggregate of primary grains. New grains (A) are widely dispersed. Large-scale bulging results in grain interpenetration (B). Straight grain-boundary segments terminating at both ends in 120° triple junctions (C) indicate the scale of γ-GBM; which is comparable to the scale of the smallest bulges. Sample 50LM900 (44.4 MPa, 900 °C).

boundary in stress/grain-size space that separates the region of dominant γ-GBM from the region of dominant ρ-GBM, known as the D_{min} line (Platt and Behr, 2011). The minimum bulge size is the minimum scale length $L\rho$ for ρ-GBM (and hence the upper limit for D_{min}), and the largest grain-boundary that has been modified by γ-GBM is the maximum scale length $L\gamma$ for γ-GBM (and hence the lower limit for D_{min}). As discussed later, the actual situation turns out to be more complicated.

3. Results

The microstructural data are shown in Table 1 and Figs. 5–6. Dynamically recrystallized grain size is plotted as a function of the final stress during deformation in Fig. 5a, and color coded for temperature. Samples showing dominant GBM microstructure are identified by solid red symbols in Fig. 5a; all others show dominant BLG/SGR microstructures.

Valcke et al. (2014) made the case that the microstructures were developed at the time of peak stress, and that the dynamically recrystallized grain size and subgrain size should be plotted against this value. We have chosen to use final stress rather than peak stress, for the following reasons. First, the proportion of recrystallized grains increased by a factor of 5 or more during deformation (Valcke et al., 2014), so that most of the new grains seen in the samples were formed near the end of the experiments, at close to the final stress. Secondly, most samples show clear evidence for dynamic recovery in the form of subgrains. Dynamic recovery should continually adjust the dislocation density, which is the driver for both the SGR and BLG mechanisms of recrystallization. Hence the new grains formed near the end of the experiments should reflect the stress at that time, rather than the peak stress. We made an exception for one sample: 36LM900. This sample was deformed to a high natural strain of 0.90 by means of three subsequent experiments, removing the sample twice from the deformation apparatus, and putting it back after re-polishing and re-jacketing (ter Heege et al., 2002; Valcke et al., 2014). The peak stress determined on this sample was 33.9 MPa, and the stress at the end of each step was 33.5, 31.9 and 26.2 MPa. Our microstructural measurements were made on the sample at the highest strain, but the grain size we measured in that sample appears inconsistent with the measured stress at the end of the experiment, as judged by the data from all the other samples of our study. The stress at the end of the final step was ~20% lower than that during the main part of the experiment, which casts doubt on the reliability of the final stress value in light of our goals. ter Heege et al. (2002) performed three other experiments at the same conditions as applied for experiment 36LM900. The average final stress of these three experiments was 34.4 MPa, and we have used this value for the plots.

For comparison, we also show dynamically recrystallized grain size data produced in large strain torsion experiments on Carrara marble by Barnhoorn et al. (2004) in Fig. 5a. The experiments by Barnhoorn et al. (2004) were conducted on essentially the same material, but at shear strain rates of 6×10^{-5} to 3×10^{-3} s^{-1}, a confining pressure of 300 MPa and temperatures of 500–727 °C. Shear strain at the end of these experiments ranged from 2.2 to 36.5. Estimated stresses were corrected for the strength of the iron jacket used for the experiments. The final stress measured at high strain was used to plot the data, and ranges from 81.4 to 291 MPa (expressed as differential stress, calculated by multiplying the shear stress by √3, as discussed by Barnhoorn et al., 2004). Grain-size measurements were made optically on ultrathin

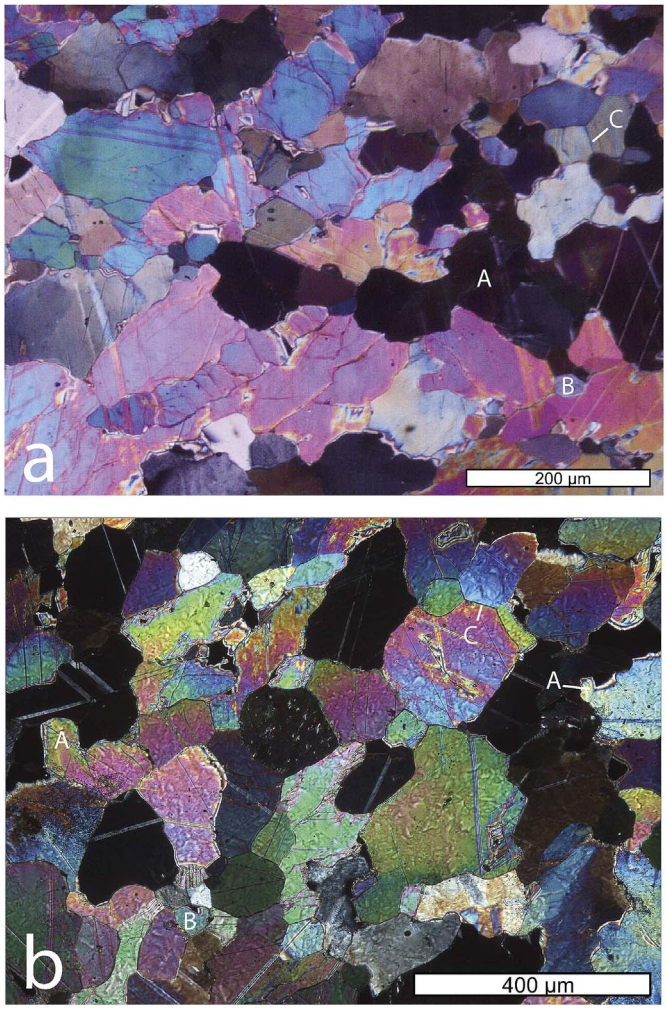

Fig. 4. Low stress microstructures. a) GBM-type microstructure with large interpenetrating primary grains (e.g., A). New grains (B) are widely dispersed. Straight grain-boundary segments (C) indicate the scale of γ-GBM. Sample 23LM900 (21.8 MPa, 900 °C). b) Low stress high-T microstructure. Large grains are relict primary grains, with boundaries locally modified by large-scale bulging (A). New grains (B) are widely dispersed. Straight grain-boundary segments (C) indicate the scale of γ-GBM. Sample 15LM950 (14.6 MPa, 962 °C).

sections, with no stereological correction, and hence can be compared directly with ours.

Taken together, our data and that from Barnhoorn et al. (2004) define a clear relationship between grain size D and differential stress σ. The relationship appears to be independent of temperature over the full experimental range from 500 to 1000 °C. The data were regressed on a log/log plot using principal component analysis, giving the relationship $D = K\sigma^{-p}$, with K = 1243 (confidence interval CI 667 to 2577) and p = −1.09 (CI −1.27 to −0.95). These results can be compared with the results from Barnhoorn et al. (2004): K = 2141 (CI 1571 to 2916), p = −1.22 (CI -1.49 to −1.03). The slopes are the same within uncertainty, and the 95% confidence intervals for the intercepts overlap, so that the values are comparable.

In Fig. 5b, we show our data and that from Barnhoorn et al. (2004) together with data from two other studies: dynamically recrystallized grain sizes measured using EBSD by Valcke et al. (2014), and data on rotation recrystallization from experimentally deformed Carrara marble published by Rutter (1995).

Grain sizes measured by Valcke et al. (2014) using EBSD on some of the same samples that we used are shown in Fig. 5b, but we have plotted them using the final stress from the experiments, whereas in their paper they used the peak stress. In most cases, the mean grain sizes are significantly less than those reported here from the same samples, and their array clearly does not lie on the same regression line. This difference suggests either that we have included a significant number of larger grains in our count, or that they included a significant number of smaller grains, or both. A possible explanation is that some of the larger recrystallized grains in the samples show evidence of internal deformation under EBSD, and hence were excluded by Valcke et al. (2014), but were included by us. The data of Valcke et al. (2014) may also have included a "tail" of very small grains detectable by EBSD but not measurable optically.

The measurements by Rutter (1995) were carried out optically on ultra-thin sections using the linear intercept technique. In many samples he identified two distinct populations of recrystallized grains, one produced by rotation (SGR), and the other by migration (GBM); he suggested that the GBM population formed by growth of grains nucleated by SGR. We were not able to find bimodal populations of recrystallized grains in our samples, and the only samples showing GBM microstructures are those deformed at the highest temperatures and lowest stresses, and they lie close to the same regression line as the others (Fig. 5a). While some grains identified by Rutter (1995) as forming by GBM may have grown from grains nucleated by SGR, we suspect that part of the larger grain-size population may be relics of the predeformational grain population. This interpretation is suggested by examination of his Fig. 5, which shows the larger grains modified and partly recrystallized by grain-boundary bulging and subgrain rotation. If this is the case, the large grains from the bimodal populations would not correctly represent a set of recrystallized grains. For this reason, only grains identified by Rutter (1995) as forming by rotation are included in Fig. 5b. Interestingly, these measurements fit well to the same stress/grain size relationship as ours and those of Barnhoorn et al. (2004).

Subgrain sizes measured as part of this study are plotted in Fig. 6a, together with the dynamically recrystallized grain sizes measured in the same samples. The data show that the measured subgrain sizes are similar to or slightly smaller than dynamically recrystallized grain sizes in the same sample; the measurements are generally within error of each other. A regression line through the combined subgrain/new grain data set in Fig. 6a has a slope of −1.33 (CI −0.88 to −2.13). Given the large uncertainty, this value does not have much significance, but it is consistent with the slope estimated for dynamically recrystallized grain size in Fig. 5.

The minimum size $L\rho$ of viable bulges for each sample, as discussed in the Methods section, is plotted in Fig. 6b, together with the maximum scale length $L\gamma$ for γ-GBM. The pairs of measurements are linked on the plot. The measurements for each sample are very similar, and for most samples, $L\gamma$ is slightly larger than $L\rho$. As discussed above, we would expect the opposite: the two measurements should bracket the D_{min} line, with $L\rho$ being larger than $L\gamma$. The discrepancy is probably a result of stochastic variations of dislocation density within the sample, perhaps due to differing orientations, and hence relative strength due to differences in the Schmid factor of different calcite grains, or due to varying amounts of dynamic recrystallization. The minimum bulge size is likely to occur in areas of maximum dislocation density, whereas the maximum scale length for γ-GBM is likely to occur in areas of minimum dislocation density. The two measurements should nevertheless give an indication of the value of D_{min} predicted by the average dislocation density for the sample in question. A regression line through the combined data set in Fig. 6b has a slope of −1.6 (CI -1.28 to −2.03). The uncertainty is large, but it is clear that both the bulge size and the scale length for γ-GBM deviate significantly from the values predicted by the regression line (dashed) for the dynamically recrystallized grain size.

4. Discussion

Our dynamically recrystallized grain size measurements, combined with the data of Barnhoorn et al. (2004), define a fairly precise

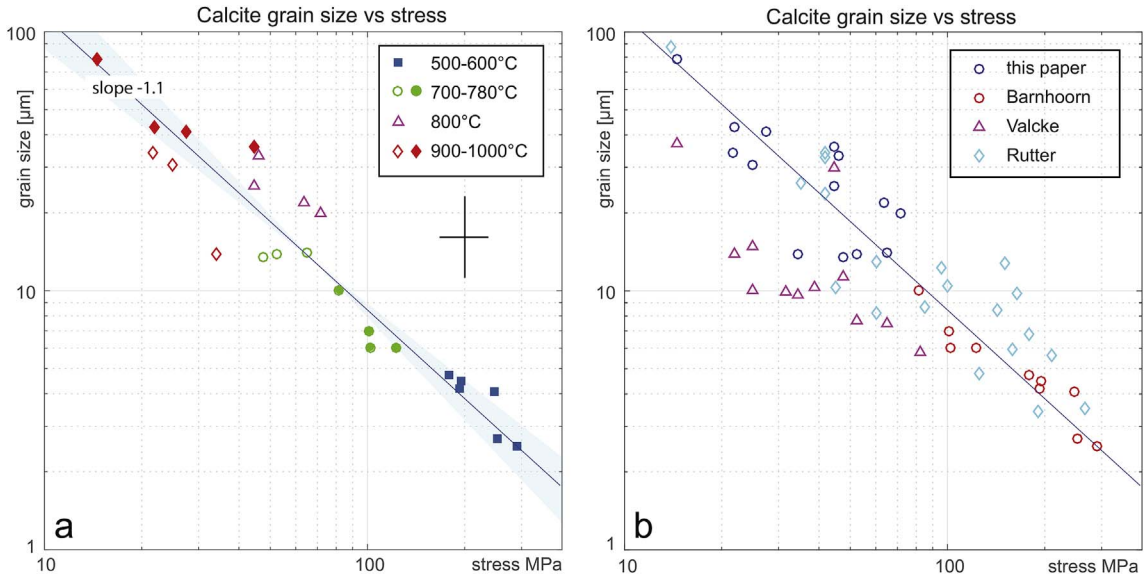

Fig. 5. Log-log plots showing dynamically recrystallized grain-size as a function of stress. a) Data are color-coded by temperature. Solid green and blue symbols are data from torsion experiments by Barnhoorn et al. (2004); open symbols are from this study. Solid red symbols are from this study and show GBM microstructures, others show BLG and SGR microstructures. The slope of the orthogonal regression line is the stress exponent of the grain-size stress relationship. Pale blue band shows the uncertainty on the slope. Cross represents average uncertainties: the standard deviation on the grain-size measurements, and the difference between the peak stress and final stress in the experiments. b) Data are color coded by author, including the measurements by Valcke et al. (2014) on the samples presented in this paper, and "rotation" data from Rutter (1995). See text for discussion. Regression line from (a) shown for reference.

piezometer for calcite, which is in turn consistent with the measurements for rotation recrystallization by Rutter (1995). This result appears to validate the optical method of grain-size measurement. Our grain sizes are consistently larger than those determined by Valcke et al. (2014) using EBSD on the same samples, however. This result does not invalidate the use of EBSD to measure grain size in general; Cross et al. (2017), for example, obtained essentially the same results using EBSD as Stipp and Tullis (2003) did using optical methods on the same set of experimentally deformed quartz samples. A possible reason for the difference between our results and those of Valcke et al. (2014) may be the different criteria that we used for distinguishing recrystallized grains from the dissected remnants of the primary grains. Valcke et al. (2014) used the lack of internal lattice distortion and subgrains as a consistent, rigorous, and objective criterion for distinguishing recrystallized grains, whereas we used microstructural criteria such as the proximity and similarity in size of new grains to subgrains and grain-boundary bulges in adjacent primary grains. The difference in the results may reflect a systematic bias towards the smallest new grains imposed by the criteria used by Valcke et al. (2014). The spacing of subgrain walls reflect dislocation density, and hence stress, so that the smallest dynamically recrystallized grains are less likely to contain subgrain walls. Similarly, the degree of lattice bending reflects the density of geometrically necessary dislocations, and hence smaller grains will show smaller angular mismatches within the grain. Both

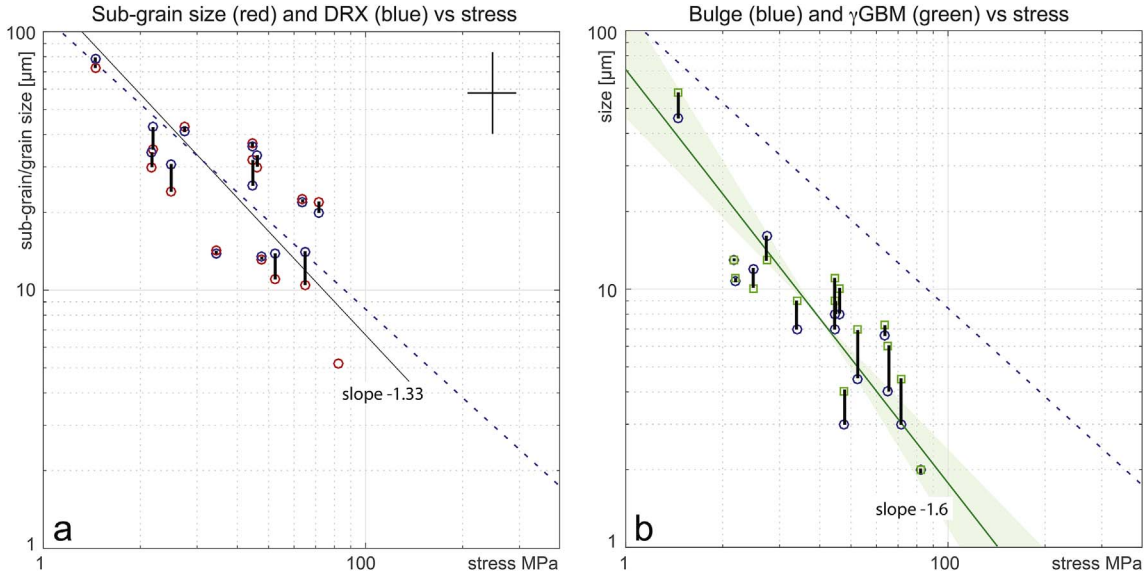

Fig. 6. a) Log-log plot showing subgrains (red symbols) and dynamically recrystallized grain size (blue symbols). Cross represents average uncertainties. Data pairs from the same samples are linked by black lines. Note the similar sizes of subgrains and new grains from the same samples. Regression line with slope −1.33 has large uncertainty. Regression line for dynamically recrystallized grain size from Fig. 5a (dashed blue line) is shown on both plots for reference. b) Minimum bulge size $L\rho$ (blue) and maximum scale length $L\gamma$ for γ-GBM (green). Data pairs from the same samples are linked by black lines. The measurements taken together define a best-fit line with a slope of ~1.6 (pale green band shows the uncertainty on the slope).

factors will result in larger grains being eliminated by the criteria used by Valcke et al. (2014). It is also possible that the smaller grains are younger, which would also explain the lack of internal deformation. In view of the lack of evidence for post-nucleation growth of recrystallized grains reported by both Valcke et al. (2014) and us, this explanation seems less likely.

The stress/grain size relationship defined by the data appears to be independent of temperature over the range 500–1000 °C. This result has implications for theories that relate dynamically recrystallized grain-size to the rate of energy dissipation (e.g., Austin and Evans, 2007, 2009), to the field boundary between grain-size sensitive and grain-size insensitive creep (e.g., De Bresser et al., 2001), or to a balance between grain-size reduction and grain growth (e.g., Derby, 1992; Shimizu, 1998). All these processes may involve a temperature dependence related to the activation energies for creep and grain-boundary migration, or in the case of the field boundary hypothesis, the difference in the activation energies of the creep mechanisms involved.

A lack of temperature sensitivity for the piezometric relationship is implied by the theoretical relationships and experimental data discussed by Twiss (1977, 1986), and was reported by Stipp and Tullis (2003) from experimental work on quartz. De Bresser et al. (2001), on the other hand, report a temperature dependence for stress-DRX data from the Mg-Al alloy Magnox, and ter Heege et al. (2005) observed a temperature dependence for the stress-DRX relationship for polycrystalline halite. Our data suggest that for calcite no detectable dependence on temperature exists.

Our measurements of subgrain size suggest that the dynamically recrystallized grain size in a given sample is within the error of (but on average slightly larger than) the size of the optically visible subgrains. These subgrains have the largest misorientations with their hosts, and hence are closest to evolving into new grains. This result suggests that subgrains play an important role in dynamic recrystallization, via both the SGR nucleation mechanism, and because subgrain boundaries are likely to control the scale of bulges involved in the BLG mechanism (Platt and Behr, 2011). This conclusion in turn provides a simple explanation for the approximately inverse linear relationship between dynamically recrystallized grain size and stress, which has been established on theoretical grounds for subgrains (Twiss, 1986; Humphreys and Hatherly, 2004). It also suggests that grain growth has not played a significant role in dynamic recrystallization at the stresses and temperatures imposed on these samples. Given the short time scale of the experiments, we cannot rule out the possibility that grain-growth plays a role in the development of dynamically recrystallized grain size in natural samples deformed over time periods many orders of magnitude longer, but we can say that the experiments do not provide evidence for this behavior.

Our measurements of the minimum size of bulges and the maximum scale length for γ-GBM provides some experimental confirmation of the concept of the D_{min} line. The measurements show large variance, but regression indicates a slope of around −1.6 on a log-log plot, which is significantly steeper than the piezometric line. The data are therefore consistent with the idea that the D_{min} line should have a stress exponent greater (~2) than that of the piezometric line (Platt and Behr, 2011).

5. Conclusions

Dynamically recrystallized grain sizes from optical measurements on experimentally deformed Carrara marble show a dependence on differential stress, but not on temperature. Taken together with previously published data, they define a paleopiezometer with a stress exponent of −1.09. This is close to the theoretical value for the spacing of sub-grain walls, which suggests that subgrain size may be the controlling factor for the size of grains nucleated by both the SGR and BLG mechanisms. The measured grain sizes are significantly larger than those previously determined using EBSD, based on the criterion that new grains should lack internal lattice distortion or substructure. This criterion may systematically bias the results to smaller grain sizes, as the angular misorientation is less in smaller grains for the same dislocation density.

Subgrain sizes measured in the same samples are closely similar in size to new grains, suggesting that new grains have not grown significantly after nucleation. This interpretation, together with the lack of temperature dependence in the stress/grain-size relationship, casts some doubt on theories of dynamic recrystallization involving grain growth, at least in the case of calcite.

Minimum bulge size, and the maximum scale length for surface-energy driven grain-boundary migration, measured on each sample define a relationship to stress with an exponent of ~1.6. This value is consistent with the idea that a line in stress-grain-size space, with an exponent larger than the piezometer, separates a region of dominant strain-energy-driven grain-boundary migration at high stress, from a region of dominant surface-energy-driven grain-boundary migration at low stress.

Acknowledgements

This research was supported in part by NSF grant EAR-0809443 awarded to J.P. Platt. We thank Andrew Cross and Eric Rybacki for their thorough and constructive reviews, and William Dunne for careful editorial handling.

References

Austin, N.J., Evans, B., 2007. Paleowattmeters: a scaling relation for dynamically recrystallized quartz grains. Geology 35, 343–346.
Austin, N.J., Evans, B., 2009. The kinetics of microstructural evolution during deformation of calcite. J. Geophys. Res. 114, B09402.
Barnhoorn, A., Bystricky, M., Burlini, L., Kunze, K., 2004. The role of recrystallization on the deformation behaviour of calcite rocks: large strain torsion experiments on Carrara marble. J. Struct. Geol. 26, 885–903.
Cross, A.J., Prior, D.J., Stipp, M., Kidder, S., 2017. The recrystallized grain size piezometer for quartz: an EBSD-based calibration. Geophys. Res. Lett. 44, 6667–6674.
De Bresser, J., Urai, J., Olgaard, D., 2005. Effect of water on the strength and microstructure of Carrara marble axially compressed at high temperature. J. Struct. Geol. 27, 265–281.
De Bresser, J.H.P., Peach, C.J., Reijs, J.P.J., Spiers, C.J., 1998. On dynamic recrystallization during solid state flow: effects of stress and temperature. Geophys. Res. Lett. 25, 3457–3460.
De Bresser, J.H.P., Ter Heege, J.H., Spiers, C.J., 2001. Grain size reduction by dynamic recrystallization: can it result in major rheological weakening? Int. J. Earth Sci. 90, 28–45.
Derby, B., 1992. Dynamic recrystallization: the steady state grain size. Scr. Metall. Mater. 27, 1581–1586.
Halfpenny, A., Prior, D., Wheeler, J., 2006. Analysis of dynamic recrystallization and nucleation in a quartzite mylonite. Tectonophysics 427, 3–14.
Herwegh, M., Poulet, T., Karrech, A., Regenauer-Lieb, K., 2014. From transient to steady state deformation and grain size: a thermodynamic approach using elasto-visco-plastic numerical modeling. J. Geophys. Res. 119, 900–918.
Hirth, G., Tullis, J., 1992. Dislocation creep regimes in quartz aggregates. J. Struct. Geol. 14, 145–160.
Humphreys, F.J., Hatherly, M., 2004. Recrystallization and Related Annealing Phenomena, second ed. Elsevier Science Ltd, Oxford, UK.
Jung, H., Karato, S.-I., 2001. Effects of water on dynamically recrystallized grain-size of olivine. J. Struct. Geol. 23, 1337–1344.
Karato, S., 1988. The role of recrystallization in the preferred orientation of olivine. Phys. Earth Planet. Interiors 51, 107–122.
Karato, S., Toriumi, M., Fujii, T., 1980. Dynamic recrystallization of olivine single crystals during high-temperature creep. Geophys. Res. Lett. 7, 649–652.
Kellermann Slotemaker, A., De Bresser, J., 2006. On the role of grain topology in dynamic grain growth–2D microstructural modeling. Tectonophysics 427, 73–93.
Kidder, S., Hirth, G., Avouac, J.P., Behr, W., 2016. The influence of stress history on the grain size and microstructure of experimentally deformed quartzite. J. Struct. Geol. 83, 194–206.
Lloyd, G.E., Farmer, A.B., Mainprice, D., 1997. Misorientation analysis and the formation and orientation of subgrain and grain boundaries. Tectonophysics 279, 55–78.
Pieri, M., Burlini, L., Kunze, K., Stretton, I., Olgaard, D.L., 2001a. Rheological and microstructural evolution of Carrara marble with high shear strain: results from high temperature torsion experiments. J. Struct. Geol. 23, 1393–1413.
Pieri, M., Kunze, K., Stretton, I., Olgaard, D.L., Burg, J.P., Wenk, H., 2001b. Texture development of calcite by deformation and dynamic recrystallization at 1000 K during torsion experiments of marble to large strains. Tectonophysics 330, 119–140.
Platt, J.P., Behr, W.M., 2011. Grainsize evolution in ductile shear zones: implications for strain localization and the strength of the lithosphere. J. Struct. Geol. 33, 537–550.

Post, A., Tullis, J., 1999. A recrystallized grain size piezometer for experimentally deformed feldspar aggregates. Tectonophysics 303, 159–173.
Prior, D.J., Boyle, A.P., Brenker, F., Cheadle, M.C., Day, A., Lopez, G., Peruzzo, L., Potts, G.J., Reddy, S., Spiess, R., Timms, M.E., Trimby, P., Wheeler, J., Zetterström, L., 1999. The application of electron backscatter diffraction and orientation contrast imaging in the SEM to textural problems in rocks. Am. Mineralogist 84, 1741–1759.
Prior, D.J., Mariani, E., Wheeler, J., 2009. EBSD in the earth sciences: applications, common practice and challenges. In: Schwartz, A.J., Kumar, M., Adams, B.L., Field, D.P. (Eds.), Electron Backscatter Diffraction in Materials Science. Springer, US, New York, NY, USA, pp. 345–360.
Rutter, E.H., 1995. Experimental study of the influence of stress, temperature, and strain on the dynamic recrystallization of Carrara marble. J. Geophys. Res. 100, 24651–24663.
Schmid, S.M., Paterson, M.S., Boland, J.N., 1980. High temperature flow and dynamic recrystallization in Carrara marble. Tectonophysics 65, 245–280.
Shimizu, I., 1998. Stress and temperature dependence of recrystallized grainsize: a subgrain misorientation model. Geophys. Res. Lett. 25, 4237–4240.
Siemes, H., Rybacki, E., Klingenberg, E., Rosière, C.A., 2011. Development of a recrystallized grain size piezometer for hematite based on high-temperature torsion experiments. Eur. J. Mineral. 23, 293–302.
Stipp, M., Tullis, J., 2003. The recrystallized grain size piezometer for quartz. Geophys. Res. Lett. 30 (2088) 3-1-3-5.
Stipp, M., Tullis, J., 2006. Effect of water on the dislocation creep microstructure and flow stress of quartz and implications for the recrystallized grain size piezometer. J. Geophys. Res. Solid Earth 11, B04201.
ter Heege, J.H., De Bresser, J.H.P., Spiers, C.J., 2002. The influence of dynamic recrystallization on the grain size distribution and rheological behavior of Carrara marble deformed in axial compression. In: De Meer, S., Drury, M.R., De Bresser, J.H.P., Pennock, G.M. (Eds.), Deformation Mechanisms, Rheology and Tectonics: Current Status and Future Perspectives, pp. 331–353.
ter Heege, J.H., De Bresser, J.H.P., Spiers, C.J., 2005. Dynamic recrystallization of wet synthetic polycrystalline halite: dependence of grain size distribution on flow stress, temperature and strain. Tectonophysics 396, 35–57.
Twiss, R.J., 1977. Theory and applicability of a recrystallized grain size paleopiezometer. Pure Appl. Geophys. 115, 227–244.
Twiss, R.J., 1986. Variable sensitivity piezometric relations for dislocation density and subgrain diameter and their relevance to olivine and quartz. In: Mineral and Rock Deformation: Laboratory Studies- the Paterson Volume. AGU Geophysical Monograph, vol. 36. pp. 247–261.
Valcke, S., Drury, M., De Bresser, J., Pennock, G., 2007. Quantifying heterogeneous microstructures: core and mantle subgrains in deformed calcite. Mater. Sci. Forum 550, 307–312.
Valcke, S., Pennock, G., Drury, M., De Bresser, J., 2006. Electron backscattered diffraction as a tool to quantify subgrains in deformed calcite. J. Microsc. 224, 264–276.
Valcke, S.L.A., De Bresser, J.H.P., Pennock, G.M., Drury, M.R., 2014. Influence of deformation conditions on the development of heterogeneous recrystallization microstructures in experimentally deformed Carrara marble. In: Faulkner, D.R., Mariani, E., Mecklenburgh, J. (Eds.), Rock Deformation from Field, Experiments and Theory: a Volume in Honour of Ernie Rutter. Geological Society London Special Publications, pp. 175–200.
van der Wal, D., Chopra, P., Drury, M., Fitz Gerald, J.D., 1993. Relationship between dynamically recrystallized grain size and deformation conditions in experimentally deformed olivine rocks. Geophys. Res. Lett. 20, 1479–1482.
White, S., 1976. The effects of strain on the microstructures, fabrics and deformation mechanisms in quartzites. Philos. Trans. R. Soc. 283A, 69–86.